J. Fluid Mech. (1973), *vol.* 57, *part* 2, *pp.* 229–240
Printed in Great Britain

An investigation of internal gravity waves generated by a buoyantly rising fluid in a stratified medium

By T. I. McLAREN, A. D. PIERCE,† T. FOHL‡ AND B. L. MURPHY

Mt. Auburn Research Associates, Inc., Newton, Massachusetts

(Received 5 June 1972 and in revised form 16 October 1972)

Experiments have been carried out to examine the spectrum of internal gravity waves excited in a stratified incompressible fluid during stabilization following the buoyant rise of a miscible fluid. The rise time of the buoyant fluid to its stabilization height in the stratified fluid was observed to be about 0·85 of the Brunt–Väisälä period for the stratified fluid. The motion of specific fluid elements in the wave field was observed using neutrally buoyant marker particles, and the particle trajectories were found to be in close accord with theoretical predictions. Observations on the internal waves generated by the forced oscillation of a spherical body suspended in the stratified medium showed the wave pattern to be well behaved and similar to that described by Mowbray & Rarity. However, the gravity wave field generated by the motion of the buoyant fluid was observed to be inhomogeneous and transient in nature. Wave periods from one to four times the Brunt–Väisälä period were clearly observed and at later times it appeared that the motion tended towards vertical oscillations at the Brunt–Väisälä frequency.

1. Introduction

This paper describes the results of an experimental investigation of the excitation of internal gravity waves in a stratified incompressible fluid, owing to the motion of a buoyantly rising miscible fluid. In the experiments, trajectories of specific fluid elements in the wave field were determined by observing the motion of neutrally buoyant marker particles. This provided information on phase relations, displacement amplitudes and time periods for the wave motion.

In one series of experiments, internal waves were generated by the motion of a solid bobbing sphere. This excited waves at a distinct frequency. In a second series of experiments, waves were generated by the motion of a buoyant fluid and in this case waves were excited over a band of frequencies. The experimental observations were in close accord with theoretical predictions.

Large-scale buoyant motions are a likely source for acoustic–gravity waves in the atmosphere. Tolstoy & Lau (1971) have studied the excitation of long-period

† Permanent address: Department of Mechanical Engineering, Massachusetts Institute of Technology.

‡ Present address: Sylvania Electric Products, Inc., Lighting Division, Danvers, Massachusetts.

waves by the buoyant rise of a nuclear cloud and found this mechanism to compare favourably in efficiency with wave generation by the explosion shock. Wave excitation by rising and oscillating fluid elements has recently been modelled mathematically by Pierce (1972) and he has applied the results to wave generation due to nuclear explosions. Hines (1960) has discussed the generation of internal gravity waves at ionospheric heights.

While internal-wave excitation by steadily rising or oscillating solid objects is well understood (Mowbray & Rarity 1967*a*, *b*; Hurley 1969; Warren 1960), excitation by buoyant fluid motions is not. The buoyant flow is too complex for simple theoretical treatment during the time when wave excitation is most important, i.e. the time when the buoyant rise has ceased and the motion becomes oscillatory (Pierce & Coroniti 1966; Morton, Taylor & Turner 1956). The principal purpose of the present work is to provide experimental data on the wave motion excited by buoyantly rising miscible fluid masses in a stratified fluid.

There have been several experimental studies of internal gravity waves excited by the collapse of a region of uniform density surrounded by a stratified fluid (Wu 1969; Schooley & Hughes 1972). The present experiment is the first to our knowledge in which the wave excitation mechanism begins with a buoyant-rise phase. It is also the first experiment in which the trajectories of fluid elements in the gravity wave field have been observed directly.

2. Experimental facility and technique

2.1. *Description of apparatus*

Figure 1 (plate 1) shows a photograph of the main experimental facility, a Plexiglas tank of dimensions $5 \times 3 \times 3\frac{1}{2}$ ft deep. This tank contains the stratified fluid, which in our experiments was a solution of varying amounts of salt in water. Distilled water was used to improve the light transmission characteristics of the solution. The procedure for filling the tank with the density stratified solution followed that described by Saunders (1962). First a solution with the maximum density of salt was run into the tank, typically to a depth of 3 or 4 in. Next a similar volume of somewhat lower density solution was floated on top of the first. This was achieved by allowing the new solution to flow onto a thin board floating on the top surface of the liquid already in the tank so as to minimize vertical mixing. Using this technique, adjacent fluid strata with density differences of less than $\frac{1}{2}\%$ could be clearly established. The operation was then repeated with a succession of fluid strata until the desired overall density deficit from top to bottom was obtained.

After a period of some days ionic diffusion at the interfaces between successive strata smoothed out the density discontinuities and eventually provided a linear density profile in the vertical direction. The density profile was measured by carefully weighing a Teflon cylinder (300 c.c.) submerged at varying depths in the stratified fluid. A density change $\Delta\rho$ in the local average value ρ_0 could be determined to an accuracy of $\Delta\rho/\rho_0 = \Delta W/W_0$, where W_0 is the apparent weight of the Teflon cylinder suspended in the fluid. This allowed the density to be determined to within less than 0·05 %.

Experiments were conducted in a number of test fluids whose density stratification parameter α $(= -\rho_0^{-1}\partial\rho_0/\partial z)$ ranged between $5 \times 10^{-3}\,\mathrm{cm}^{-1}$ and $5 \times 10^{-4}\,\mathrm{cm}^{-1}$. Thus the Brunt–Väisälä periods $2\pi/(\alpha g)^{\frac{1}{2}}$ for the stratified fluid mixtures used in our experiments were in the range 3–10 s.

Internal gravity waves were excited in the stratified test mixture by one of two methods. In a series of preliminary experiments, a sphere was suspended in the test tank, and using a small d.c. motor was allowed to oscillate vertically at a controlled amplitude and frequency. Measurements were made of the amplitude and frequency of waves as a function of the angle from the axis of motion of the oscillating sphere. The results of these experiments are reported in § 4 below.

In the main series of experiments in this investigation a small volume of buoyant fluid was released from a control mechanism on the floor of the Plexiglas tank. The release mechanism can be refilled with buoyant fluid from beneath the tank; the buoyant fluid is then retained in a hemispherical volume by a sliding lid on top. The lid is opened using a draw cord which is led through guides on the tank floor and up the end walls of the tank to allow manual control from outside the tank. The lid is spring-loaded to allow a controlled opening time. Ethyl or methyl alcohol were generally used as the buoyant fluid owing to their low density and good miscibility with water, and in some cases the alcohol was dyed to enhance visualization of the source region.

2.2. *Visualization of internal gravity waves*

The wave fields generated in the test tank were visualized by using neutrally buoyant polystyrene beads dispersed through the stratified fluid mixture. These beads were purchased in the unexpanded state but were then thermally treated to produce varying degrees of expansion in accordance with the requirements for a particular experiment. Samples of beads within quite narrow density ranges are thus obtained and an even distribution of beads can be dispersed throughout the density stratified mixture. Wave propagation in the stratified test fluid may then be observed by examining the motion of individual beads which characterize the motion of the surrounding fluid.

The wave field created is a three-dimensional one, albeit cylindrically symmetric, and in order to simplify the interpretation of data, observations were made on a thin two-dimensional characteristic section of the wave field. This was done by conducting the experiments in a darkened laboratory with a collimated light beam illuminating only a thin vertical section of the test fluid through the axis of symmetry for the experiment. The polystyrene beads act as excellent light scattering centres and their movements were recorded using a 16 mm cine camera.

3. Theory

The theory of the propagation of waves in an incompressible stratified fluid has been presented by a number of authors (Pierce 1963; Tolstoy 1963; Gille 1966) and will not be repeated here. A theoretical exposition directed specifically

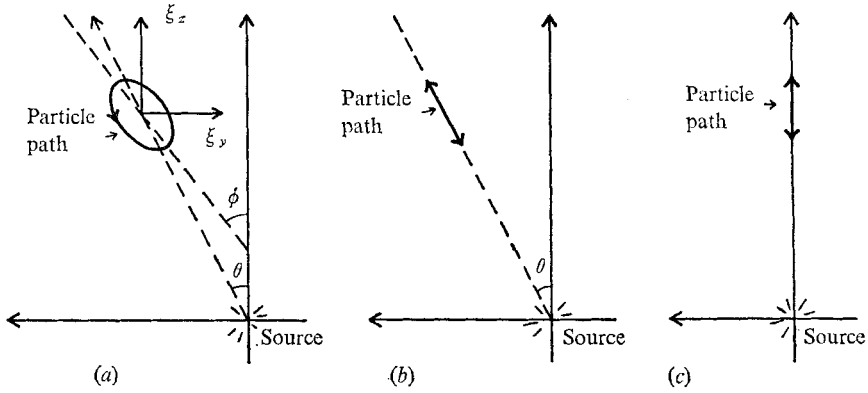

FIGURE 2. Illustrations of predicted particle trajectories in internal gravity wave. (*a*) General case; (*b*) $\omega = \omega_0 \cos\theta$; (*c*) $\omega = \omega_0$.

towards the analysis of data from the present experiments is also available in an earlier report (Kahalas, McLaren & Murphy 1972). It is known that, for propagation of internal gravity waves, one must have $\omega_0^2 \cos^2\theta < \omega^2 < \omega_0^2$, where ω is the gravity-wave angular frequency, ω_0 the Brunt–Väisälä frequency and θ the direction of wave propagation with respect to the vertical. The particle trajectories for specific fluid elements in the gravity wave can be written as

$$(\delta^2+\gamma^2)\,\xi_x^2+\alpha^2\xi_z^2-2\alpha\gamma\xi_x\xi_z=\alpha^2\delta^2, \tag{1}$$

where ξ is the particle displacement, and the co-ordinate system has been chosen so that $\xi_y = 0$. The parameters α, δ and γ are given by

$$\alpha=\frac{1}{\omega}\frac{\omega_0^2-\omega^2}{\omega_0^2 C_{gx}}A, \quad \gamma=\frac{\omega_0^2-\omega^2}{\omega\omega_0^2}\frac{C_{gz}}{C_{gx}^2}A, \tag{2a,b}$$

$$\delta=-\frac{1}{\omega_0^2-\omega^2}\frac{\omega_0^2}{2g}A, \tag{2c}$$

where C_{gx} and C_{gz} are the group-velocity components in the x and z directions and A is an amplitude factor.

Equation (1) is the equation of an ellipse. As illustrated in figure 2(*a*), the direction of the major axis of this ellipse is in general not coincident with the group-velocity vector $\mathbf{C}_g$. The inclination ϕ of the major axis of the ellipse to the vertical may be defined, with the restriction $(0 < \phi < \frac{1}{2}\pi)$, by

$$\tfrac{1}{2}\tan 2\phi=\gamma\alpha/(\delta^2+\gamma^2-\alpha^2), \tag{3}$$

and the ratio L_2/L_1, where L_2 and L_1 are the semi-major and semi-minor axes of the ellipse, respectively, may be written as

$$\frac{L_2^2}{L_1^2}=\frac{(\alpha^2+\gamma^2+\delta^2)\cos 2\phi+(\delta^2+\gamma^2-\alpha^2)}{(\alpha^2+\gamma^2+\delta^2)\cos 2\phi-(\delta^2+\gamma^2-\alpha^2)}. \tag{4}$$

It can also be shown that

$$\tfrac{1}{2}\tan 2\phi=\frac{\omega_0^2-\omega^2}{2\omega^2-\omega_0}\cot\theta. \tag{5}$$

Theoretical arguments not presented here indicate that a source of frequency ω (where $\omega < \omega_0$) radiates strongly near the angle $\theta = \pm \cos^{-1}(\omega/\omega_0)$ (Pierce 1963; Hurley 1969). At precisely this angle, the group velocity is zero. However, at angles only slightly less in magnitude than this value, the group velocity has a finite value and the amplitude is expected to be relatively large. For $\omega^2 \simeq \omega_0^2 \cos^2\theta$ (5) reduces to

$$\tan 2\phi = \tan 2\theta, \tag{6}$$

which is satisfied by

$$\phi = \theta. \tag{7}$$

Equation (4) may be simplified and in general can be written as

$$\frac{L_1^2}{L_2^2} = \frac{\cos 2\phi + 1 - (2\omega^2/\omega_0^2)}{\cos 2\phi - 1 + (2\omega^2/\omega_0^2)}. \tag{8}$$

Thus in the case where $\omega^2 \to \omega_0^2 \cos^2\theta$, then $L_1 \to 0$ and the particle trajectory becomes a straight line in the direction of θ ($= \phi$); see figure 2(*b*).

In the special case of $\theta \simeq 0$, the only propagating frequency is ω_0, so $L_1 \to 0$, and $\phi = 0$. Since the straight-line orbits are in the direction of ϕ they will thus be aligned in the vertical direction; see figure 2(*c*). At the other extreme case of horizontal propagation, as $\theta \to 90°$, ϕ may tend to either 0 or 90°, depending on whether ω^2 is less than or greater than $\frac{1}{2}\omega_0^2$, and elliptical trajectories should in general be observed in the horizontal direction.

Combining (5) and (8) we can eliminate ω^2/ω_0^2 to obtain

$$\tan\theta = \frac{1}{\sin 2\phi}\,\frac{1+(L_1/L_2)^2}{1-(L_1/L_2)^2} - \cos 2\phi. \tag{9}$$

Thus if one measures ϕ and the ratio L_2/L_1 for an observed particle trajectory, it is possible to compute θ without explicitly taking the frequency into account. (This presumes $0 < \theta < 90°$, $0 < \phi < 90°$.)

It is also possible to predict the sense in which particles move around elliptical orbits. If the source is to the lower left of the observer, the orbits appear to be clockwise. In a similar manner, the orbits would be counterclockwise if the source were to the lower right (Pierce 1965).

4. Results

4.1. *Bobbing-sphere experiments*

A series of preliminary experiments was carried out employing an oscillating sphere as the localized disturbance in a stratified fluid. A schematic illustration is presented in figure 3. Spheres 0·5–2·5 in. diameter were used and oscillation frequencies from approximately one-third to one times the Brunt–Väisälä frequency were examined. A 16 mm cine camera recorded the movement of the sphere and the wave patterns indicated by the particle motions, viewing only a vertical two-dimensional plane as described in § 2.

Analysis of the data consisted of plotting the movement of the neutrally buoyant beads at various locations in the wave field. The wave pattern was clearly observed to take the form of symmetrical 'jet' regions on either side of

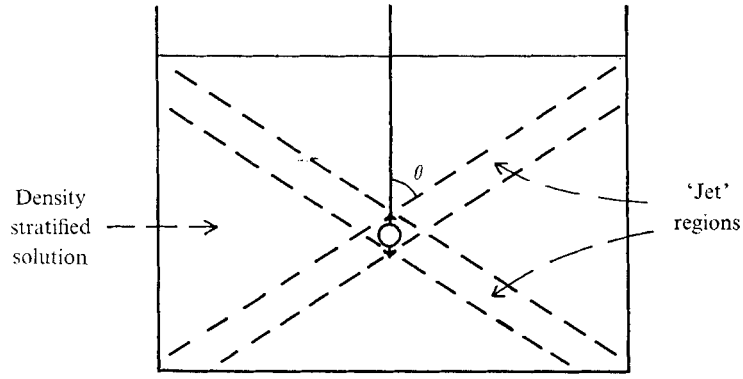

FIGURE 3. Schematic diagram for bobbing-sphere experiment.

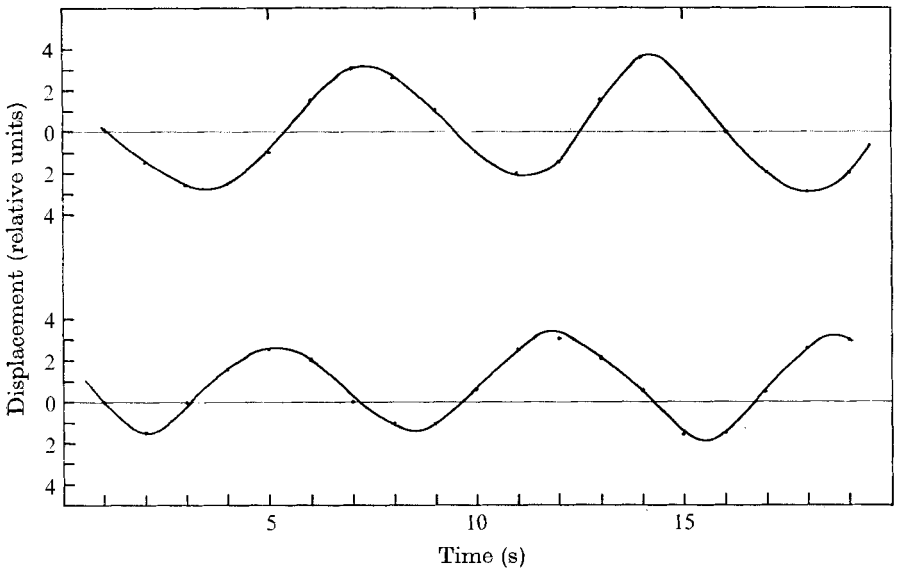

FIGURE 4. Displacement/time plots for two particles in the gravity-wave jet in bobbing-sphere experiment. Both particles are at same radial distance from sphere but are separated azimuthally. Note the phase difference.

the oscillating source, in the shape of a cross, as reported by Mowbray & Rarity (1967*a*). The angle of inclination of the gravity-wave jet regions was found to vary closely as $\theta = \cos^{-1}(\omega/\omega_0)$ for values of $\omega < \omega_0$, where θ is the jet inclination to the vertical. This is consistent with Hurley's (1969) results based on the theory of an oscillating cylinder in a stratified fluid.

All the particles in the jet region were found to follow straight-line paths, and figure 4 shows displacement/time plots for two such particles in the gravity-wave jet, spaced azimuthally but at equal radial distances from the oscillating source. These clearly indicate the phase change across the jet dimension, and the aggregation of such data points across the jet at a fixed radial distance from the source gives a measurement of the wavelength. In our experiments this wavelength was found to agree to within 15 % with the diameter of the oscillating source region,

which was defined as the sphere diameter plus the amplitude of the imposed oscillation. The wave amplitude seems to fall off with increasing distance R from the source approximately as $1/\sqrt{R}$ as might be anticipated on consideration of energy conservation.

Measured periods for all particles within the gravity-wave jet regions agree closely with the known source periods. The average angle of inclination of the gravity-wave jet regions, defined by the bounds within which measurable particle displacements were observed, and also the inclination of the straight-line particle paths, correlated closely with the value of $\cos^{-1}\omega/\omega_0$ for the respective experiments. This is consistent with the theoretical prediction of straight-line trajectories aligned in the group-velocity direction when $\omega = \omega_0 \cos\theta$.

4.2. *Buoyant-release experiments*

A number of experiments were carried out to visualize the wavelength generated by the motion of a buoyantly rising volume of fluid in a stratified environment. Most of the data analysed were for experiments where a small test volume of alcohol was released at the tank bottom into a stratified salt solution whose stratification parameter α was $5 \times 10^{-4}\,\mathrm{cm}^{-1}$. The same visualization technique was employed as described above, a cine film being taken of the motion of neutrally buoyant beads in a two-dimensional vertical plane passing through the release point of the buoyant fluid.

Owing to the rapid entrainment by the buoyant fluid of the heavier brine solution, stabilization of the rising fluid tended to occur at relatively low levels in the test tank. Thus observations were mainly made on the upward-directed waves, which provided a longer wave path before reflexions at the tank side walls or the top surface of the stratified fluid interfered with the observations.

In contrast with the bobbing-sphere experiments, where an observer could clearly distinguish the wave 'jet' regions of the wave field, in the case of a buoyant fluid release the wave pattern appeared to be considerably more complex. General observations were made on a number of buoyant releases and some were analysed in detail; results are presented below.

Distribution of gravity-wave frequency. In the case of the bobbing-sphere experiments, the period for all particles observed within the wave jet region appeared to be constant and equal to the sphere oscillation frequency, within the scatter of the measurements. With the buoyant-fluid release, however, a wide spectrum of wave frequencies was observed. No discernible gravity-wave motions were detected during the rise of the buoyant fluid. The waves observed seemed to be generated after the rise, emanating from the oscillatory motion of the fluid around its stabilization height. Particle trajectories were plotted for various parts of the wave field and these showed periods varying from the Brunt–Väisälä period to three to four times this for waves propagating at angles close to the horizontal. It became difficult to resolve waves with periods longer than this which may propagate at even shallower angles, but there was evidence of a non-periodic motion in the horizontal direction, possibly associated with the horizontal spread of the buoyant plume at the stabilization height.

The main reason for the differences between the wave fields generated by the

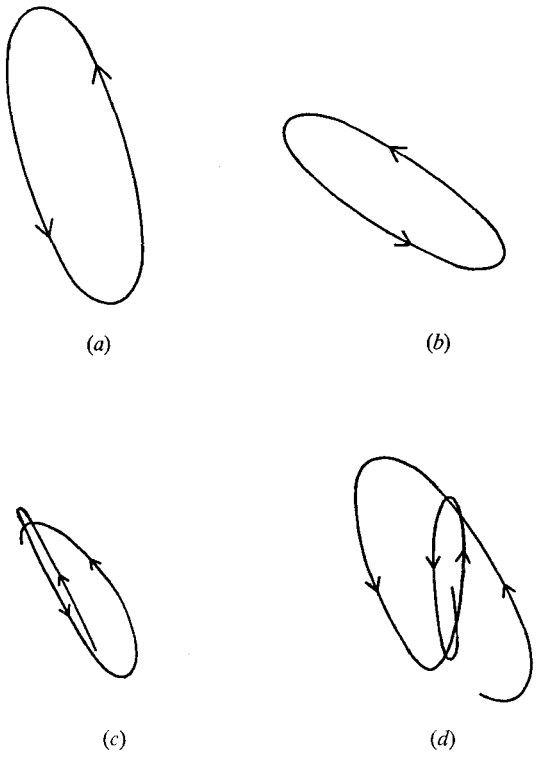

FIGURE 5. Particle trajectories from analysis of buoyant-release experiment. (*a*), (*b*) and (*c*) are from the same experiment; (*d*) is at a late time for another experiment.

bobbing sphere and by the buoyant release is that the source region in the latter case represents an extended and transient source. As a result, for the buoyant release, the trajectory of an individual particle in the wave field may be observed to vary non-periodically in time. For example, a particle executing an elliptical orbit may subsequently change to a different elliptical orbit, or may for a time be observed to follow a straight-line path. Figure 5 shows sketches of some actual particle trajectories recorded for a buoyant-release experiment.

The overall observation time for most of our buoyant-release experiments was usually four or five times the Brunt–Väisälä period for the stratified fluid. The buoyantly rising test fluid appeared to stabilize after about two oscillations, although an extensive volume of the stratified fluid in the stabilization region tended to continue oscillations at about the Brunt–Väisälä frequency for longer times. Our observation time lasted typically for two or three Brunt–Väisälä periods after stabilization of the buoyant fluid. Towards the end of this observation time there were generally indications, and in one experiment very clear evidence, that the particle motions eventually tended to straight-line paths in the vertical direction at the Brunt–Väisälä period. Such a case is illustrated by the particle trajectory in figure 5 (*d*). It is not clear whether this is the result of (i) the motion of the extended source region tending towards this period, or (ii) a result of the fact that the strongest later arrivals from a broad-band transient

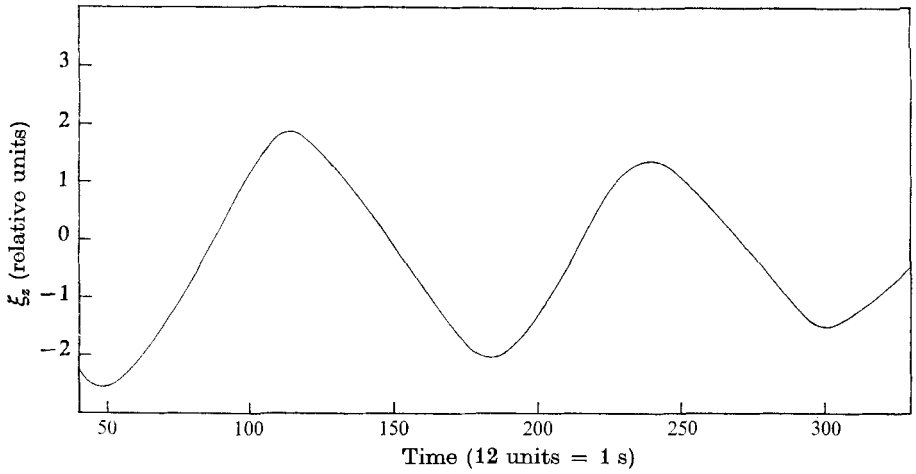

FIGURE 6. Gravity-wave vertical amplitude ξ_z as a function of time for a field point in a buoyant-release experiment. Within this observation time the wave period has changed from 11·7 s to 10·0 s.

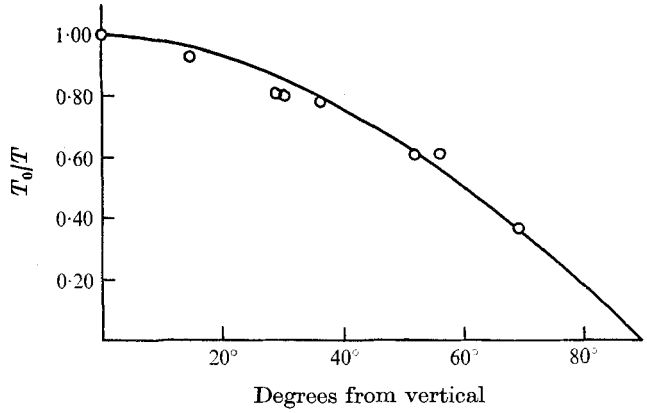

FIGURE 7. T_0/T as a function of particle path inclination to the vertical for straight-line trajectories observed in buoyant-release experiment. Solid curve is $\cos^{-1}(T_0/T)$. T_0 is the Brunt–Väisälä period; T is the observed period.

source should be at the Brunt–Väisälä frequency since the group velocity goes to zero with zero slope at that frequency.

Figure 6 shows the vertical component of particle displacement as a function of time for the particle trajectory shown in figure 5(*d*). The particle period has changed from 11·7 s for the first half cycle to 10·0 s for the last half-cycle. This latter value is approximately the Brunt–Väisälä period for the stratified fluid (9·8 s). The vertical trajectory at $\omega \simeq \omega_0$ is also consistent with the theoretical predictions. A more detailed analysis of the displacement period in terms of group-velocity (dispersion) arguments is precluded by the fact that the source is spatially extended and has a complex space–time behaviour.

The direction of the particle motions around their elliptical orbits was observed to be clockwise or counterclockwise in agreement with theoretical expectations.

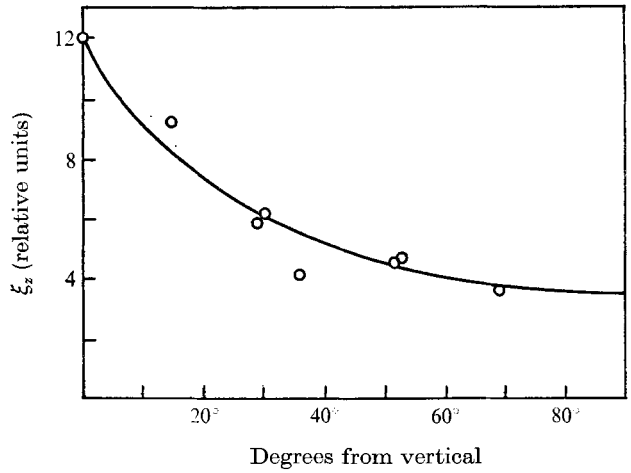

FIGURE 8. Gravity-wave vertical amplitude ξ_z as function of azimuthal angle for fixed radial distance in buoyant-release experiments.

It follows from (8) that, if a particle trajectory is a straight line (i.e. $L_1 = 0$), then $\omega^2 = \omega_0^2 \cos\phi$. This is borne out by the data presented in figure 7, where the data points relate only to particles observed to be executing straight-line paths in the wave field generated by a buoyant-fluid release.

In the more general case of an elliptical particle trajectory, such as that shown in figure 5(*a*), ϕ and L_1/L_2 may be measured. Then equation (9) provides the value of θ which indicates the direction of the source region. From a number of such observations the location of the source may of course be determined from the intersection of the θ lines. In our experiments the volume dimensions of the oscillating source region are not specifically defined and it was not possible to assess critically the accuracy of θ values calculated from (9). However, in general the predicted values were in good agreement with expectations based on a knowledge of the general location of the source region. Quantitative correlation was difficult because our observation field extended only to about eight or ten times the source region dimensions.

Description of gravity-wave amplitude. Owing to the transient nature of the gravity-wave field generated in a buoyant-release experiment, it was not feasible to confirm the decay of amplitude with increasing distance from the source region, as was done for the bobbing-sphere experiments. However, the data gave no indication that the decay should differ markedly from the $1/\sqrt{R}$ form observed in the bobbing-sphere experiments.

Data were obtained to indicate the variation of the gravity-wave amplitude with the azimuthal angle. Figure 8 presents data showing the variation of the vertical component of the gravity-wave amplitude with azimuthal angle. This vertical displacement is proportional to the potential energy in the wave. It is seen that the vertical displacement is a maximum directly above the oscillating source region (where, however, the group velocity C_g falls to zero for the only propagating frequency ω_0) and falls to a minimum in the horizontal direction.

Rise time to stabilization. Table 1 shows the results of the measurements made

Release number	Measured rise time, T_R (s)	T_R/T_0
11–3	8·0	0·82
11–4	8·3	0·85
11–5	8·3	0·85
12–2	8·0	0·82
12–3	8·3	0·85
12–5	8·3	0·85
12–6	8·0	0·82
12–7	9·0	0·92

TABLE 1. Rise time to stabilization of buoyant-fluid releases

of the rise time for buoyant releases. The rise time is defined as the time interval from release of the buoyant fluid until the top surface of the stabilizing fluid is first observed to fall back in an oscillation about the stabilization height. Typically the stabilizing fluid is observed to undergo about two oscillations before its vertical motion finally ceases. It is seen that the rise time appears to be about 0·85 times the Brunt–Väisälä period for the stratified fluid.

5. Conclusions

Experiments have been carried out to investigate the internal gravity waves generated in an incompressible density stratified medium (*a*) by the forced oscillation of a spherical body suspended in the stratified medium, and (*b*) by the motion of a buoyantly rising miscible fluid. The gravity wave motions were analyzed by observing the detailed motion of small neutrally buoyant beads dispersed throughout the stratified medium, and agreement was found between the observations and the theoretical predictions of earlier work (Pierce 1965). Observations were also made on the rise to stabilization of the buoyant miscible fluid, and it was found that the rise time to stabilization height was about 0·85 times the Brunt–Väisälä period for the stratified fluid.

The gravity-wave field generated by the motion of a buoyant fluid was observed to be inhomogeneous and transient in nature. However, the theory permits identification of the location of an unseen source of internal gravity waves, if measurements are made of only two characteristics of fluid particles' trajectories, namely the inclination of the major axis of particle motion, and the ratio of major to minor axis for its (in general) elliptical orbit.

This research was sponsored by the Advanced Research Projects Agency under Air Force Office of Scientific Research contract F44620-71-C-0086.

REFERENCES

GILLE, J. C. 1966 Acoustic gravity waves in the earth's atmosphere. *Florida State University, Dept. of Meterology, Tech. Note*, no. 66–7.

HINES, C. O. 1960 Internal atmospheric gravity waves at ionospheric heights. *Can. J. Phys.* **38**, 1441. (Correction in *Can. J. Phys.* **42**, 1424.)

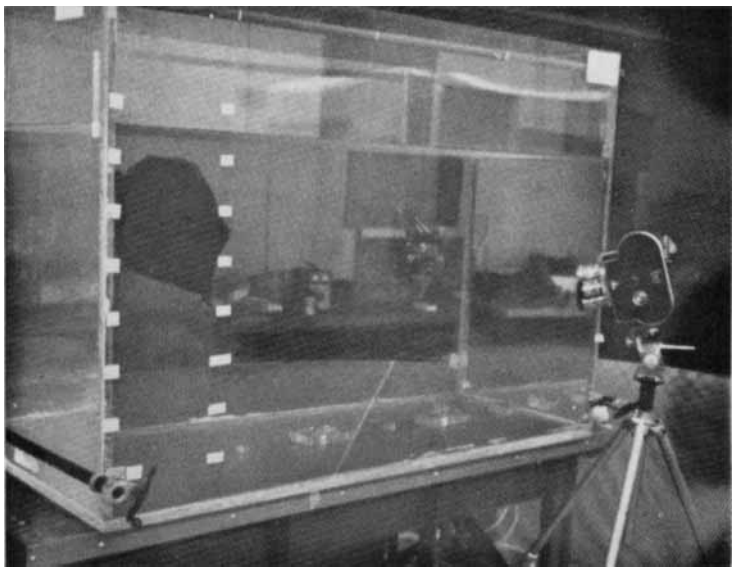

FIGURE 1. The experimental facility.

HURLEY, D. C. 1969 The emission of internal waves by vibrating cylinders. *J. Fluid Mech.* **36**, 657.

KAHALAS, S. L., MCLAREN, T. I. & MURPHY, B. L. 1972 Study of acoustic–gravity wave generation by nuclear detonations. *Final Rep. Contract* F 44620-71-C-0086.

MORTON, B. R., TAYLOR, G. I. & TURNER, J. S. 1956 Turbulent gravitational convection from maintained and instantaneous sources. *Proc. Roy. Soc.* A **234**, 1.

MOWBRAY, D. E. & RARITY, B. S. H. 1967*a* A theoretical and experimental investigation of the phase configuration of internal waves of small amplitude in a density stratified liquid. *J. Fluid Mech.* **28**, 1.

MOWBRAY, D. E. & RARITY, B. S. H. 1967*b* The internal wave pattern produced by a sphere moving vertically in a density stratified liquid. *J. Fluid Mech.* **30**, 489.

PIERCE, A. D. 1963 Propagation of acoustic–gravity waves from a small source above the ground in an isothermal atmosphere. *J. Acoust. Soc. Am.* **35**, 1798.

PIERCE, A. D. 1965 The propagation of infrasonic waves in an isothermal atmosphere with constant winds. *J. Acoust. Soc. Am.* **39**, 832.

PIERCE, A. D. 1972 A model for acoustic–gravity wave excitation by buoyantly rising and oscillating air masses. *Proc. AGARD Meeting on Effects of Acoustic–Gravity Waves on Electromagnetic Wave Propagation*, Wiesbaden, Germany. To be published.

PIERCE, A. D. & CORONITI, S. C. 1966 A mechanism for the generation of acoustic–gravity waves during thunderstorm formation. *Nature*, **210**, 1209.

SAUNDERS, P. M. 1962 Penetrative connection in stably stratified fluids. *Tellus*, **2**, 177.

SCHOOLEY, A. H. & HUGHES, B. A. 1972 An experimental and theoretical study of internal waves generated by the collapse of a two-dimensional mixed region in a density gradient. *J. Fluid Mech.* **51**, 159.

TOLSTOY, I. 1963 The theory of waves in stratified fluids including the effects of gravity and rotation. *Rev. Mod. Phys.* **35**, 207.

TOLSTOY, I. & LAU, J. 1971 Generation of long internal gravity waves in waveguides by rising buoyant air masses and other sources. *Geophys. J. Roy. Astron. Soc.* **26**, 1–4.

WARREN, F. W. G. 1960 Wave resistance to vertical motion in a statified fluid. *J. Fluid Mech.* **7**, 209.

WU, J. 1969 Mixed region collapse with internal wave generation in a density stratified medium. *J. Fluid Mech.* **35**, 531.